SUPPORTING INFORMATION

Tailoring reactive handles on the surface of nanoparticles for covalent conjugation of biomolecules

Francesca Mazzotta,[1] Sharafudhen Pottanam Chali,[1] Ingo Lieberwirth,[1] Calum Ferguson,[1,2] and Katharina Landfester*,[1]

[1]*Max Plank Institute for Polymer Research, Department of Physical Chemistry of Polymers, Ackermannweg 10 55128 Mainz, Germany*

[2]*Department of Polymer Chemistry, Birmingham B15 2TT, United Kingdom Birmingham, UK*

E-mail: landfester@mpip-mainz.mpg.de

Contents

^{1}H-NMR spectroscopy to quantify the total number of FGs

Herein, a detailed discussion of how to estimate the maximum number of FGs that can be found in a NPs based on the ^{1}H-NMR spectrum of the polymer. The ^{1}H-NMR spectrum of the purified polymer was used to determine the monomer relative ratios. For each polymer three NMR tubes were individually measured leading to a total of three spectra. For the P(BzMA-co-AEMA), in each spectrum, the CH_2 peak of the BzMA (δ = ~4.4 – 5, **c** in Figure S1A, S2B, S3B) was compared to the CH_2 peak of the AEMA (δ = ~2.6 – 3.2, **g** in Figure S1A, S2B, S3B). Specifically, the AEMA's mol % was calculated as reported in Equation S1:

$$AEMA\ mol\ \% = \frac{\frac{CH_2\_AEMA}{2}}{\frac{CH_2\_AEMA}{2} + \frac{CH_2\_BzMA}{2}} * 100 \quad \text{(S1)}$$

For the P(BzMA-co-MAA), in each spectrum, the Aromatic peak of the BzMA (δ = ~6.5 – 7.5, **c** in Figure S1B, S4B, S5B) was compared to the COOH peak of the MAA (δ = ~12.1 – 12.7, **g** in Figure S1B, S4B, S5B). Specifically, the MAA's mol% was calculated as reported in Equation S2:

$$MAA\ mol\ \% = \frac{\frac{COOH\_MAA}{1}}{\frac{COOH\_MAA}{1} + \frac{Aromatic\_BzMA}{5}} * 100 \quad \text{(S2)}$$

To determine the molar concentration relative to 1 g of system, we have introduced an "average-monomer" (AM) molecular weight (MW). In this sense, the polymer will be composed by a new "average-monomer". The molecular weight of this "average-monomer" will be dictated by the mol % of each component:

$$MW\ of\ the\ "average-monomer" = \frac{MW_{BzMA} * BzMA\ mol\ \% + MW_{FM} * FM\ mol\ \%}{100} \quad \text{(S3)}$$

where FM stands for functional monomer, either MAA or AEMA. Given the calculated mol% the MW of the AM are: 174 g/mol for P(BzMA-co-MAA) 1 wt%, 163 g/mol for P(BzMA-co-MAA) 10 wt%, 176 g/mol for P(BzMA-co-AEMA) 1 wt%, 175 g/mol for P(BzMA-co-AEMA) 10 wt%.

Given the MW of the AM, the moles of FM per gram of AM can be calculated using Equation S4:

$$Moles\ of\ FM\ per\ g\ of\ AM = [FM]mol = \frac{FM\ mol\ \%}{MW_{AM}} \quad \text{(S4)}$$

Next, it should be noted that the FM mol% is equivalent to the FG mol%. This is true given that each FM presents a single FG, either an amino or a carboxylic group. Finally, given a selected concentration of NPs (e.g. 0.1 wt% which corresponds to a solid content (SC) of 1 g/L) the concentration of FGs in solution can be calculated:

$$FGs\ concentration = [FGs] = [FM]mol * SC \quad \text{(S5)}$$

It should be noted that this method is determining the total number of FGs. The result can be also interpreted as the maximum number of FGs that can be obtained on the NPs surface. This method does not take into consideration groups that might be trapped in the NPs core or unavailable.

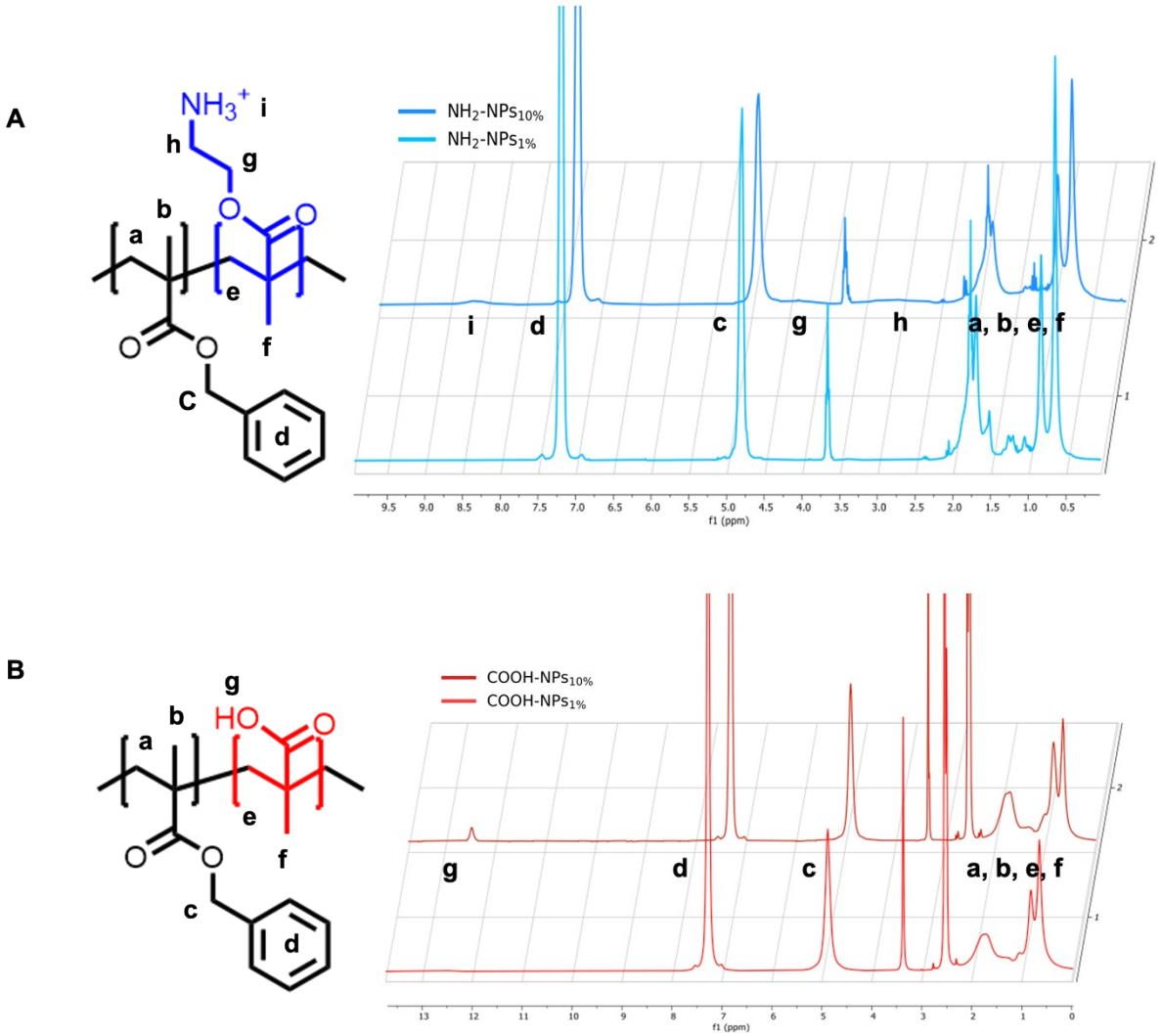

Figure S1: ^{1}H-NMR spectra of the purified P(BzMA-co-AEMA) (A) and P(BzMA-co-MAA) polymers in d6-DMSO (400 MHz, at 298 K). The peaks are labeled with the representative hydrogens within the polymer.

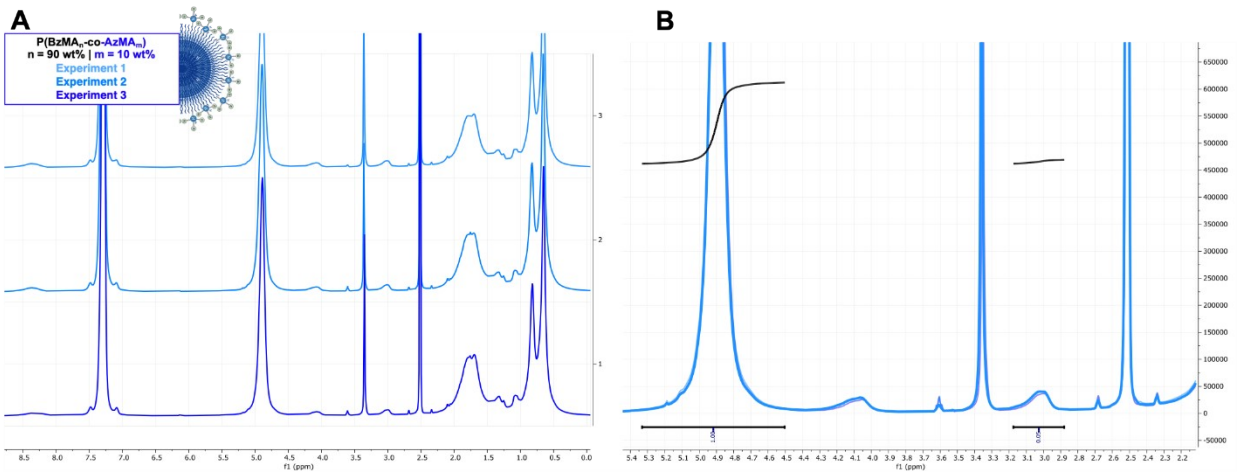

Figure S2: (A) ^{1}H-NMR spectra of the purified P($BzMA_{90\ wt\%}$-co-$AEMA_{10\ wt\%}$)in d6-DMSO (400 MHz, at 298 K). (B) Close up on the regions of interest where the normalized integrals of the BzMA ($\delta \sim 4.9$) and AEMA ($\delta \sim 3$) CH_2 peaks are reported.

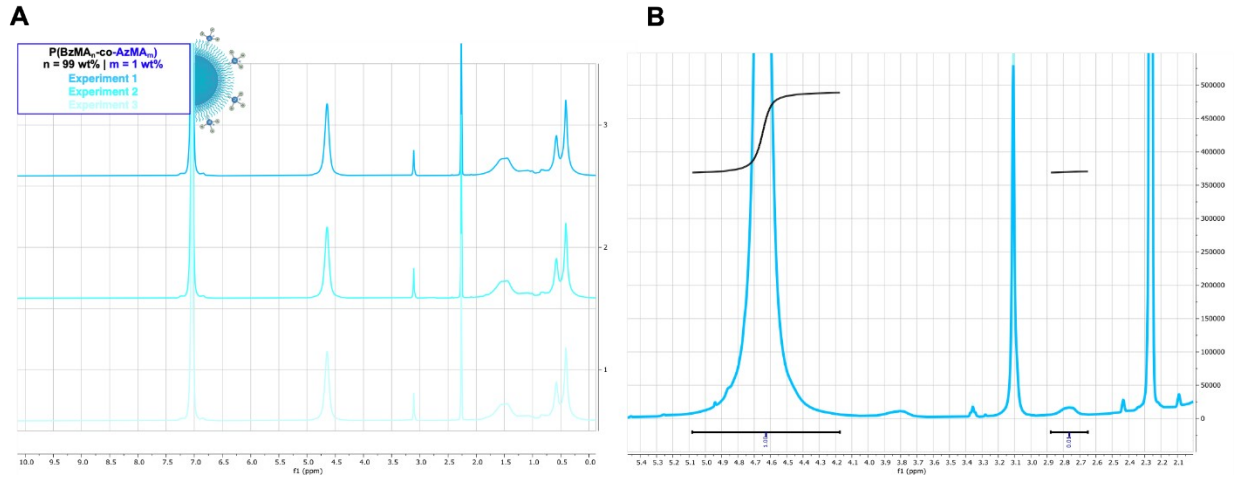

Figure S3: (A) ^{1}H-NMR spectra of the purified P($BzMA_{99\ wt\%}$-co-$AEMA_{1\ wt\%}$)in d6-DMSO (400 MHz, at 298 K). (B) Close up on the regions of interest where the normalized integrals of the BzMA ($\delta \sim 4.9$) and AEMA ($\delta \sim 3$) CH_2 peaks are reported.

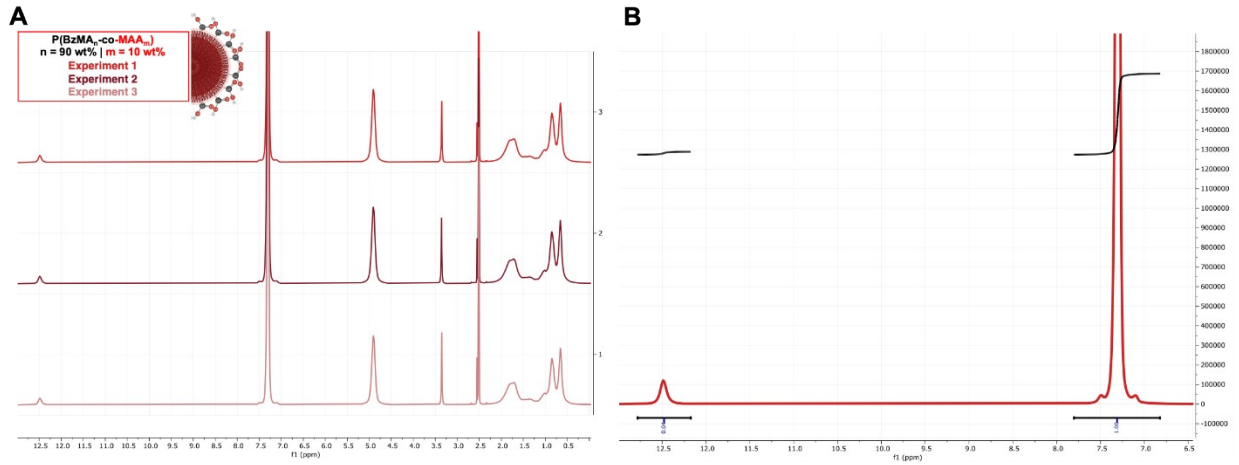

Figure S4: (A) ^{1}H-NMR spectra of the purified P(BzMA$_{90\ wt\%}$-co-MAA$_{10\ wt\%}$)in d6-DMSO (400 MHz, at 298 K). (B) Close up on the regions of interest where the normalized integrals of the COOH peak (δ ~12.5) and aromatic peak (δ ~7.3) are reported.

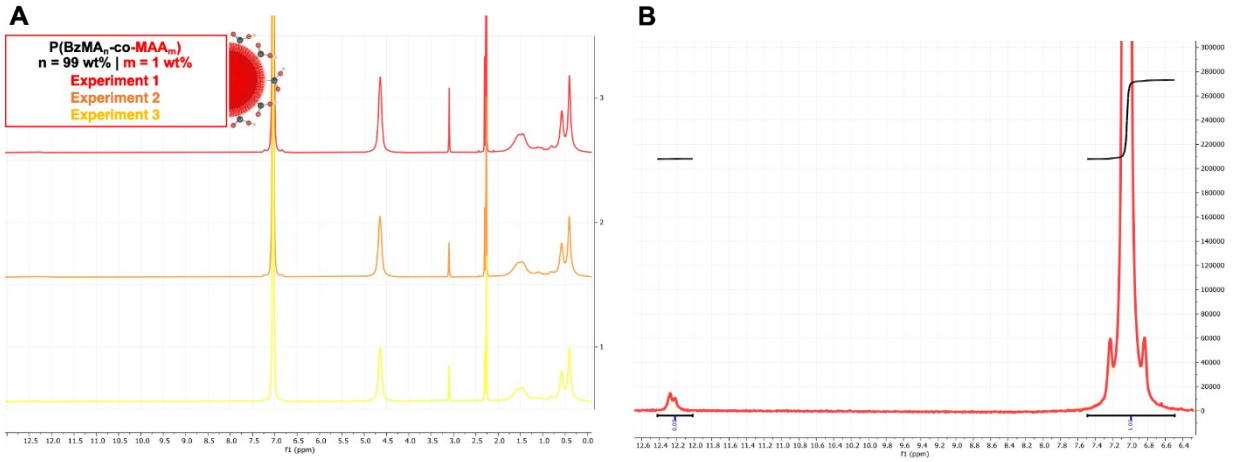

Figure S5: (A) ^{1}H-NMR spectra of the purified P(BzMA$_{99\ wt\%}$-co-MAA$_{1\ wt\%}$)in d6-DMSO (400 MHz, at 298 K). (B) Close up on the regions of interest where the normalized integrals of the COOH peak (δ ~12.5) and aromatic peak (δ ~7.3) are reported.

Table S1: Integral ranges and absolute values for each ^{1}H-NMR spectrum. The absolute values were used in Equation S1 and S2 to calculate the mol% of the correspondent FMs (Table S2).

	P(BzMA$_{99\ wt\%}$-co-AEMA$_{1\ wt\%}$)		P(BzMA$_{90\ wt\%}$-co-AEMA$_{10\ wt\%}$)	
	Range	*Absolute*	*Range*	*Absolute*
Experiment 1	5.33 .. 4.42	5.46E+08	5.32 .. 4.49	5.06E+08
	3.13 .. 2.90	7.86E+06	3.19 .. 2.90	1.83E+07
Experiment 2	5.09 .. 4.14	5.38E+08	5.31 .. 4.54	5.12E+08
	2.89 .. 2.66	8.60E+06	3.19 .. 2.86	2.25E+07
Experiment 3	5.28 .. 4.48	5.16E+08	5.33 .. 4.50	4.55E+08
	3.12 .. 2.93	7.40E+06	3.17 .. 2.88	2.15E+07
	P(BzMA$_{99\ wt\%}$-co-MAA$_{1\ wt\%}$)		P(BzMA$_{90\ wt\%}$-co-MAA$_{10\ wt\%}$)	
	Range	*Absolute*	*Range*	*Absolute*
Experiment 1	12.46 .. 12.07	3.96E+06	12.68 .. 12.16	3.82E+07
	7.64 .. 6.44	1.10E+09	7.71 .. 7.00	1.08E+09
Experiment 2	12.42 .. 12.11	4.29E+06	12.49 .. 12.00	4.35E+07
	7.56 .. 6.52	1.23E+09	7.48 .. 6.56	1.24E+09
Experiment 3	12.42 .. 12.02	5.14E+06	12.78 .. 12.17	4.17E+07
	7.49 .. 6.49	1.44E+09	7.80 .. 6.82	1.18E+09

Table S2: Quantification of mol % of BzMA or FM (and FG) in the final system for each collected NMR spectrum. The triplicates generate a mean value, and an error based on the standard devotion (STDEV). Figure 2D and 2H use these values, together with the MW of the AM, in Equation S5, to obtain the μM concentration of FG in a 0.1 wt% solution.

	P(BzMA$_{99\ wt\%}$-co-MAA$_{1\ wt\%}$)		P(BzMA$_{90\ wt\%}$-co-MAA$_{10\ wt\%}$)	
Quantification	*BzMA (mol %)*	*MAA (mol %)*	*BzMA (mol %)*	*MAA (mol %)*
Experiment 1	98.23	1.77	85.03	14.97
Experiment 2	98.28	1.72	85.04	14.96
Experiment 3	98.25	1.75	84.96	15.04
Mean mol %	98.25	1.75	85.01	14.99
STDEV	0.03	0.03	0.04	0.04
	P(BzMA$_{99\ wt\%}$-co-AEMA$_{1\ wt\%}$)		P(BzMA$_{90\ wt\%}$-co-AEMA$_{10\ wt\%}$)	
Quantification	*BzMA (mol %)*	*AEMA (mol %)*	*BzMA (mol %)*	*AEMA (mol %)*
Experiment 1	98.58	1.42	96.52	3.48
Experiment 2	98.43	1.57	95.79	4.21
Experiment 3	98.59	1.41	95.48	4.52
Mean mol %	98.53	1.47	95.93	4.07
STDEV	0.09	0.09	0.53	0.53

Table S3: From monomer to final polymer composition.

Polymer Type	BzMA wt%	FMs wt%	FM initial mol %	Polymer yield (%)	M_n g/mol^{-1}	M_w g/mol^{-1}	Đ
BzMA-AEMA	90	10	1	33	38416	109734	2.86
BzMA-AEMA	99	1	11	43	40629	113572	2.8
BzMA-MAA	90	10	2	84	38000	120382	3.17
BzMA-MAA	99	1	19	85	51323	180743	3.52

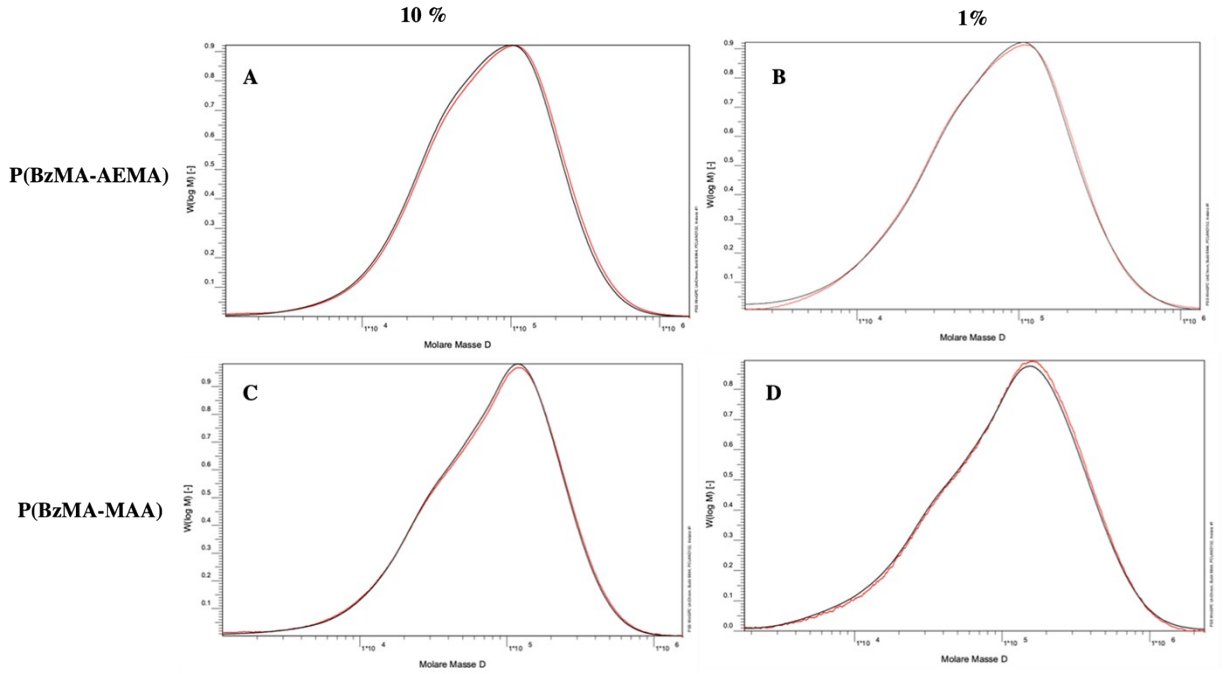

Figure S6: UV absorbance at 280 nm (red) and RI (red) spectrum obtained via GPC for the (A) NH_2-NPs-10%, (B) COOH-NPs-10%, (C) NH_2-NPs-1% and (D) COOH-NPs.

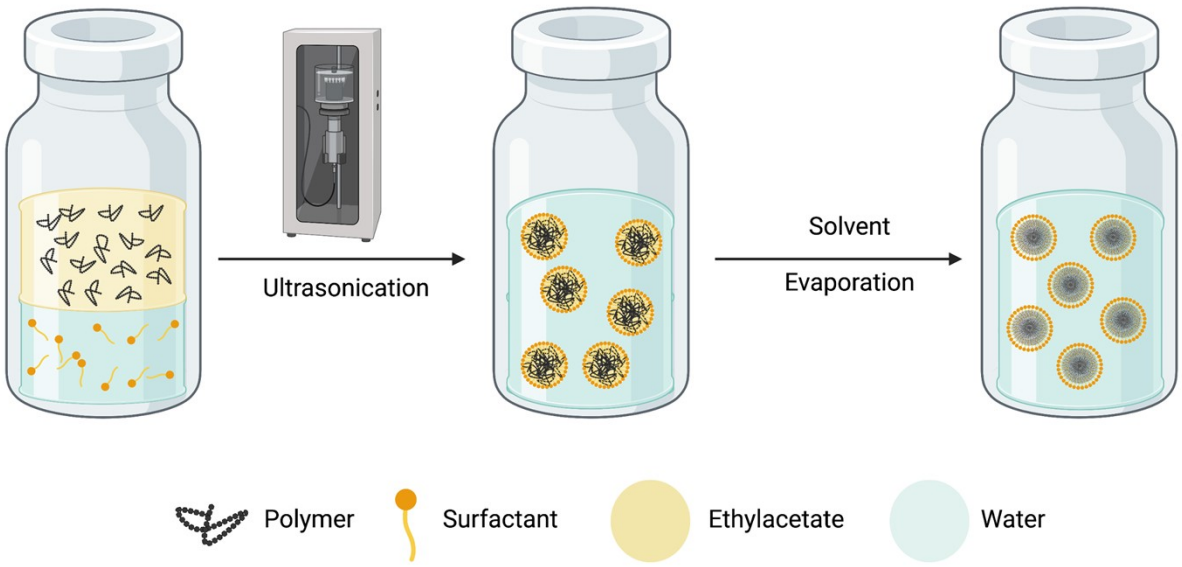

Figure S7: Schematic representation of the miniemulsion-solvent evaporation process: the polymer is dissolved in the oil phase and mixed with the aqueous phase. The ultrasonication forms the NPs which are then solidified by evaporating the oil phase.

Modification of COOH-NPs using EDC/NHS chemistry

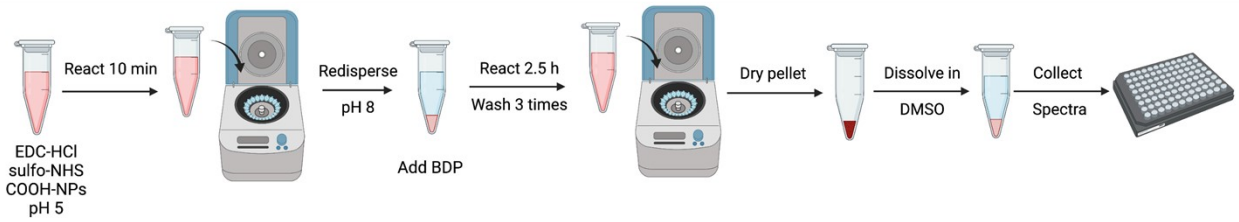

Figure S8: Schematic representation of the EDC/NHS protocol on the COOH-NPs.

The EDC/NHS conjugation required an initial screening to optimize the reaction yield. While many parameters could be investigated, we focused on determining optimal buffer conditions and reaction times (Figure S9) resulting in the need for a two-step reaction (carboxylic activation at pH 5 and amino addition at pH 8) and a 2.5 h reaction time. Additionally, the proper EDC and NHS concentrations were investigated (Figure S9), finding that a 14.4 mM concentration was optimal to saturate the curve at lower dye concentrations. More in detail, in this work samples were prepared as follows: first the COOH-NPs were diluted to a 0.11 wt% solution in a 0.1 wt% solution of Lutensol AT50 in 10 mM PBS at (pH 5) for a final volume of 180 µL. Then EDC-HCl and sulfo-NHS were collected from their storage location (-20 ºC) and left to equilibrate at room temperature for 15 min. The chemicals were quickly weighed to obtain a large excess (14.4 mM) and dissolved with the COOH-NPs solution. To reduce hydrolysis, which would hamper the amide bond formation, the particles were left to react for only 10 min and then centrifuged for 10 min at 15.5 krcf at 4 ºC. The pellet was redispersed in 200 µL of 10 mM pH 8 PBS buffer with the proper amine (dye or protein) concentration. At this pH NHS hydrolyzes within 2.5 h thus the procedure has no need for longer reaction times.

While this screening facilitated selecting the EDC/NHS conditions, many more parameters can be screened as they could affect the reaction (e.g. temperature).

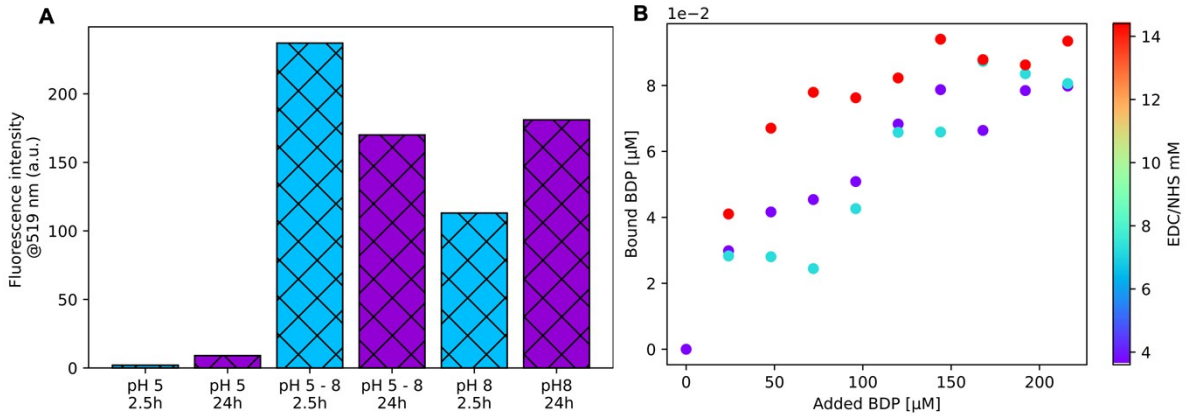

Figure S9: (A) EDC/NHS chemistry optimization, where time (2.5 h in blues and 24 h in purple) and buffer conditions were investigated. The COOH-NPs-10% were reacted with BDP in different experimental conditions, the final dried polymer was dissolved in DMSO, and the fluorescence intensity is reported in this plot. (B) BDP conjugation to COOH-NPs10% with different EDC and NHS concentrations to optimize dye conjugation conditions.

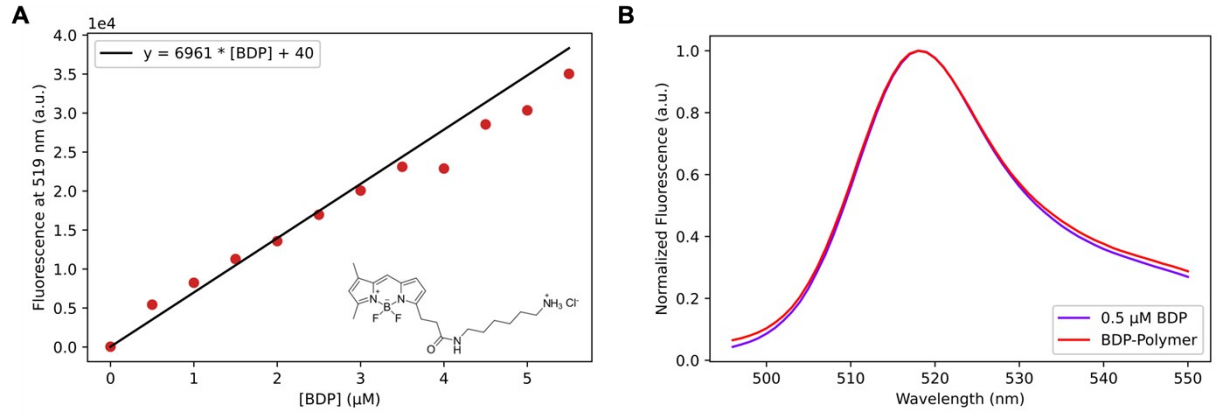

Figure S10: (A) Calibration curve of BDP in DMSO. The inset shows the chemical structure of BDP. (B) Comparison between the normalized fluorescence spectra of BDP and BDP-Polymer.

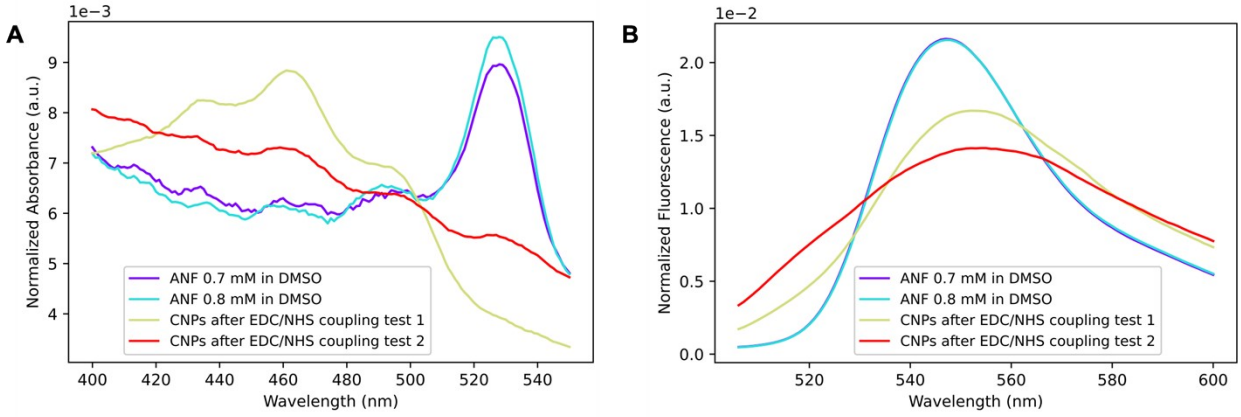

Figure S11: (A) Absorbance and (B) fluorescence spectra of ANF and ANF-polymer system showing the large difference, which hamper the dye quantification.

Modification of NH_2-NPs using EDC/NHS chemistry

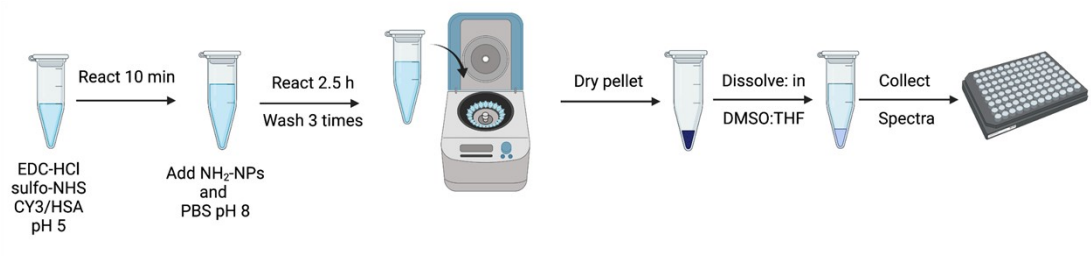

Figure S12: Schematic representation of the EDC/NHS protocol on the NH_2-NPs.

The EDC/NHS conjugation on NH_2-NPs was slightly modified compared to the COOH-NPs. First the carboxylic dye (CY3) in DMSO or the protein (HSA) was added to each of the eppendorf and diluted, to a final volume of 10 µL, to the proper concentration using 10 mM PBS (pH 5). Then EDC and NHS (1.4 mM) were weighed and dissolved in the same buffer. The conjugating reagent solution (10 µL) is then added to the dye and the samples were left to react for 10 min. In the mean time a 0.11 wt% solution of the NH_2-NPs was prepared in a 10 mM PBS pH 8 buffer solution. Lastly, 180 µL of NH_2-NPs were added to each eppendorf and were left to react for 2.5 h.

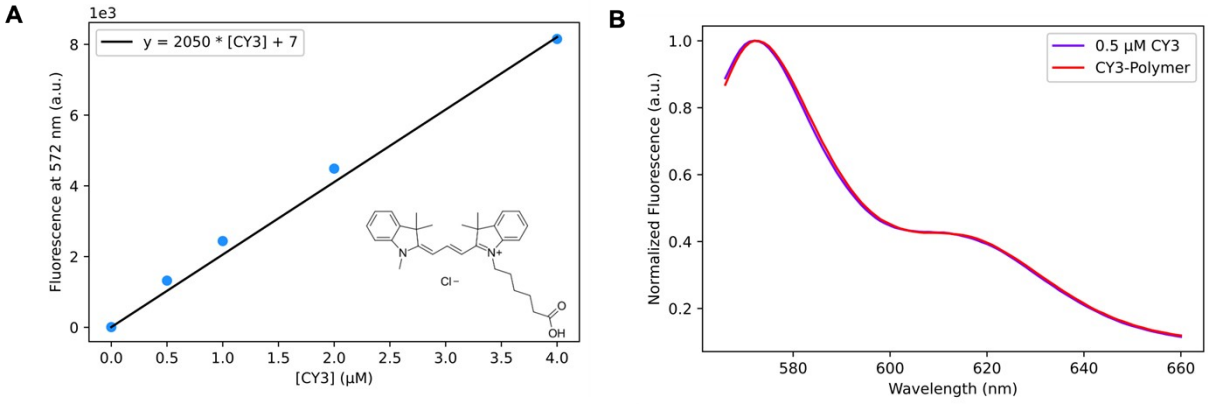

Figure S13: (A) Calibration curve of free CY3 in DMSO. The insert shows the CY3 chemical structure. (B) Comparison between the normalized spectra of CY3 and CY3-Polymer

Fluorescamine assay to quantify NH_2 groups

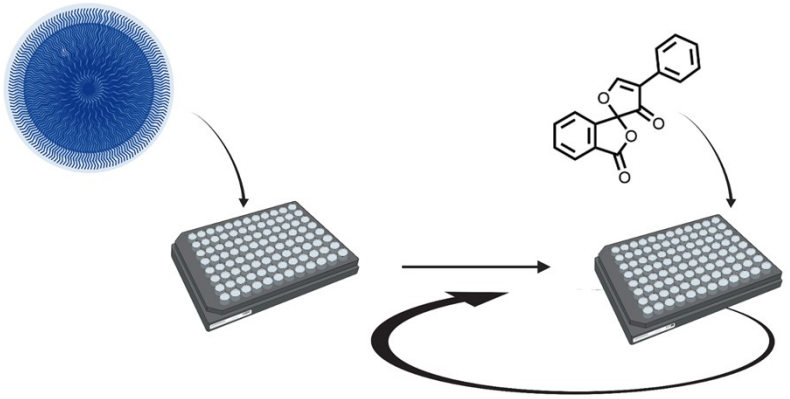

Figure S14: Schematic representation of the adapted Fluorescamine assay.

In the specific case of NH_2-NPs, often the fluorescamine assay is implemented to quantify the amino groups on different type of NPs such as silica NP,1,2 liposomes3 or polystyrene.4–6 This reaction can be of high interest due to its fast execution time, thus was tested with these NPs. The method required some adaptation as in this system the fluorescence of the fluorescamine-NPs was much stronger than the correspondent calibration curve (Figure S15 A) probably due to the particle becoming part of the chromophore4 and altering the fluorescent properties of the dye. Therefore, the NPs were titrated by subsequent addition of fluorescamine until the fluorescent signal reached a plateau.

For the analysis, the fluorescamine concentration was plotted against the fluorescence intensity at 478 nm to obtain a titration curve. The average fluorescence of the triplicates was then fitted using a Langmuir model (Equation S6).

$$Fluorescanece = \frac{a * b * [Fluorescamine]_{added}}{1 + b * [Fluorescamine]_{added}} \quad \text{(S6)}$$

The last points of the titration, where no evident fluorescence change was detected, were averaged, and used in the model to extrapolate the fluorescamine concentration which coincides with the available amino groups in a 0.01 wt% solution.

The results detected an amino concentration of 660 µM for the NPs-10% and 40 µM for the NPs-1% (Figure S15) which are higher numbers compared to the PCD and CY3 quantification results. In the first case, the difference could be associated to the fact that the method utilizes DMSO to solubilize the dye, thus the addition of the compound during the titration, might modify the outer conformation of the NPs allowing it to detect previously hidden amino groups. On the other hand, the difference compared to the EDC/NHS quantification could be associated to the different reaction yields, which for the fluorescamine conjugation should be higher (80-95%[7] based on theoretical calculations) than the EDC/NHS coupling on methacrylate-based surfaces.[8]

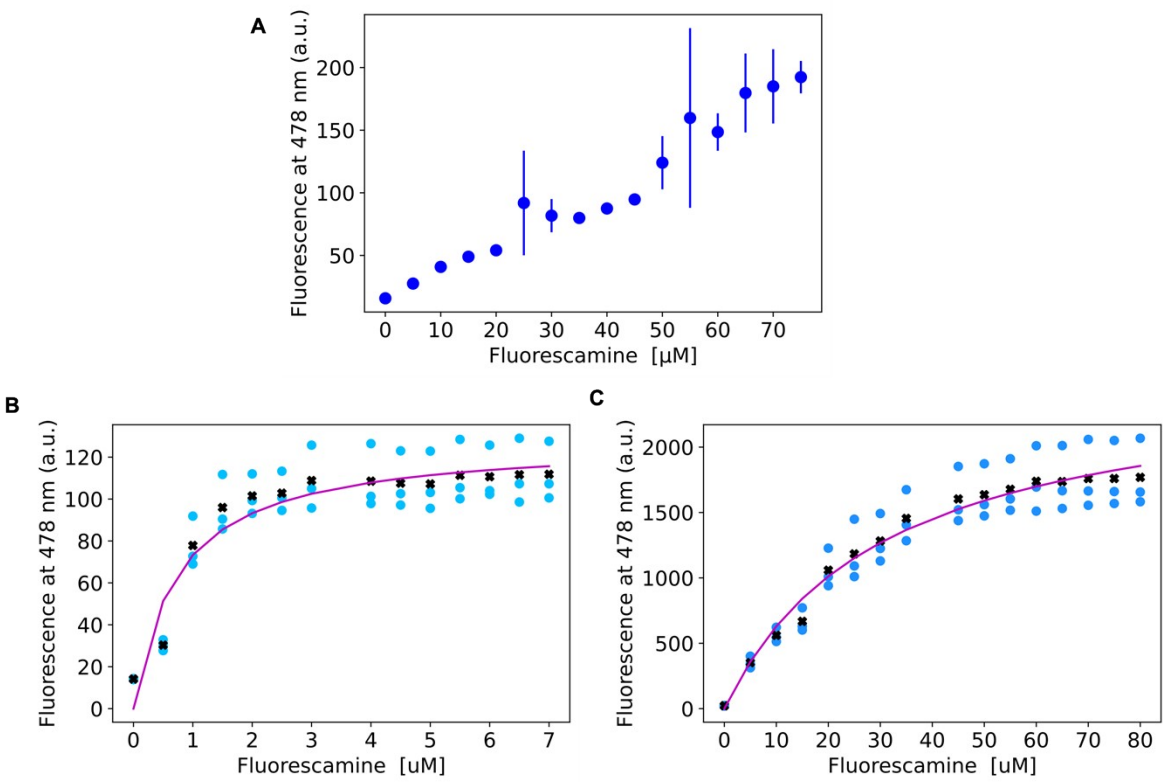

Figure S15: (A) Comparison between the fluorescence intensity in the calibration curve system (10 mM of propylamine and increasing concentration of fluorescamine) and the fluorescamine titration on (B) NH_2-NPs-1% or (C) NH_2-NPs-10% in a 0.01 wt% NPs solution. The plots report the triplicate measurement and, in black, the average result used for the quantification.

Error evaluation on μM quantification

In this section we discuss in more detail the primary errors associated to each of the quantification methods presented in this work. Notably, many errors can arise in each method, details can be found in works such as Bharti *et al.*[9] and Böckenhoff *et al*.[10] . To estimate the error each measurement has been performed in triplicates and evaluated singularly. The values reported in Figure 2D and 2H in the main text derive from the mean of the triplicate measurements and the error bars are obtained by the standard devotion of the triplicates.

Total FGs

The quantification of total of FGs is determined through the application of ^{1}H-NMR spectroscopy. Specifically, the relative molar composition between the BzMA and the FM was converted into molar concentration of FGs in a NP solution with a 1 mg/mL concentration of polymer (Equation S2). Therefore, the primary sources of error in the quantification are associated to NMR peak integration and sample reproducibility.

Firstly, the NMR peak integration is an experimental error, which is inherent to the technique itself. In this case, error can arise due to inadequate baseline correction or the broadness of the peak in selected regions. For instance, when comparing the CH_2 and aromatic signals of the BzMA, the integrals should report a 2:5 ratio. However, small variations in the selected region could lead to divergencies such as 2:4.8. Such an error would be easily detected in the CH2:BzMA ratio; yet, when comparing unknown ratios (e.g. BzMA:FM) ,this error can result in a significant variation.

The second major error is the sample reducibility. To obtain triplicate measurements, the produced polymer was introduced into three separate NMR tubes. Notably, the polymer presented here was achieved via free radical polymerization, which has poor control over the statistical polymer produced. Therefore, it is possible that each polymer chain may present large deviation not only in polymer length but also in monomer ratio. The presence of large heterogeneity in the polymer composition may result in different molar %.

Visible FGs

The quantification of visible FGs is based on the particle charge detection (PCD), which is conducted via titration method. Specifically, the volume of titrant utilized (V_{titrant}) is converted into a molar concentration in a NP solution with a 1 mg/mL concentration of polymer using Equation 1, as reported in the main text.

The degree of reproducibility is dictated by the ability of determining the V_{titrant}. It should be noted that the streaming currents[10] within the sample may affect the results of the investigation. Therefore, the discrepancies in the measurements can be considered an intrinsic experimental error.

Accessible FGs

The quantification of accessible FGs is based on a dye conjugation process. Specifically, a dye is coupled to the NPs. Unreacted dye is removed via repeated centrifugation and re-suspension steps. The final product is dissolved in an organic solvent and a fluorescence spectrum is acquired. The fluorescence signal can be converted into a dye concentration by using a calibration curve. The reaction is repeated in different conditions to obtain a titration curve where the detected dye increases until reaching a plateau. In this plateau, increasing the free dye for conjugation does not affect the amount of bound dye. Hence, averaging the values in this range enables detection of the

maximum number of dyes that can be conjugated to the NP solution. Furthermore, given that the solid content of the polymer is known in this solution, the dye concentration can be correlated to the concentration of dye in NP solution with a polymer concentration of 1 mg/mL.

The errors in this measurement derive from multiple factors, a greater number than those identified in the aforementioned methods. The errors can be attributed to various factors, including the reaction itself (e.g., yield reproducibility), cleaning steps (e.g., pipetting), calibration curve errors, and polymer interference with chromophore. The primary factors affecting the quantification are the reaction yield and the cleaning steps. In the first case, the variability of the reaction yield will result in large discrepancies in quantification, due to inherent variability in the amount of conjugated dye. Specifically, the EDC/NHS coupling is challenging[11] and requires detailed optimization of reaction conditions to improve the yield[12].

Notably, such reaction-bound error will be found in any chemical-conjugation based approach. Therefore, it is of great importance to select reactions with high yields (e.g. substitute EDC/NHS coupling with click chemistry reactions) and with limited reaction steps. However, this is not always possible and will strongly depend on the type of FGs that needs to be quantified.

Cleaning errors, on the other hand, are highly user dependent. Therefore, the direct method presented in this work stands to limit such manual limitations.

Fluorescamine Assay

Fluorescamine assay quantification was determined using titration curves. The concentration of added dye which allow the fluorescence to plateau is associated to the accessible group in the specific experimental conditions. Such determination is based on user-biased selection of the plateau point. This point is clearly detectable in the averaged values (black dots in Figure S15) but less pronounces in the individual titration curves. Therefore, in this case the error is not associated to the triplicate measurements but rather the amount of dye added between each titration point. In the presented experiment each titration point consists of a 0.5 or 5 μM fluorescamine addition, respectively for the 1% and 10% systems. These concentrations can be considered the error in the measurement. Given that the experiment was performed on a 0.01 wt% solution, the determined concentration was scaled by a factor of 10. It is then necessary to apply the same scaling factor on the error.

Table S4: Quantification of COOH and NH_2 FGs in the COOH-NPs and NH_2-NPs. The table reports the FG concentration in µM for a 0.1 wt% solution of NPs, both the mean value and the standard deviation (stdev) are reported for each triplicate set. The concentrations are obtained using NMR for the total FGs, PCD for the visible FGs, and Dye conjugation for the accessible FGs. For the NH_2-NPs Fluorescamine assay results are also reported. The values in this table are used to produce Figure 2D and 2H.

FGs [µM]		COOH-NPs-1%	COOH-NPs-10%	NH_2-NPs-1%	NH_2-NPs-10%
NMR - Total	Mean	194	1641	163	452
	Stdev	3	5	10	59
PCD - Visible	Mean	24	53	24	182
	Stdev	2	3	1	5
Dye - Accessible	Mean	0.07	0.22	0.7	17
	Stdev	0.03	0.13	0.2	2
Fluorescamine	Mean	-	-	50	600
	Stdev	-	-	5	50

Micro BCA

Micro BCA was performed following an adaptation of the publish method[13] using the Pierce Micro BCA Protein Assay Kit (Thermo Scientific). After the last step of purification, the purified NPs were re-suspended in 150 µL of MilliQ water at a final concentration of 0.13 wt%. The solution was mixed with 150 µL of the working reagent. The reaction was carried out for 2 h at 37 ºC on a thermoshaker at 500 rpm. The particles were then centrifuged for 10 min at 4 ºC with 15 krcf. 200 µL of the supernatant was collected and the absorbance was measured at 562 nm in a plate reader.

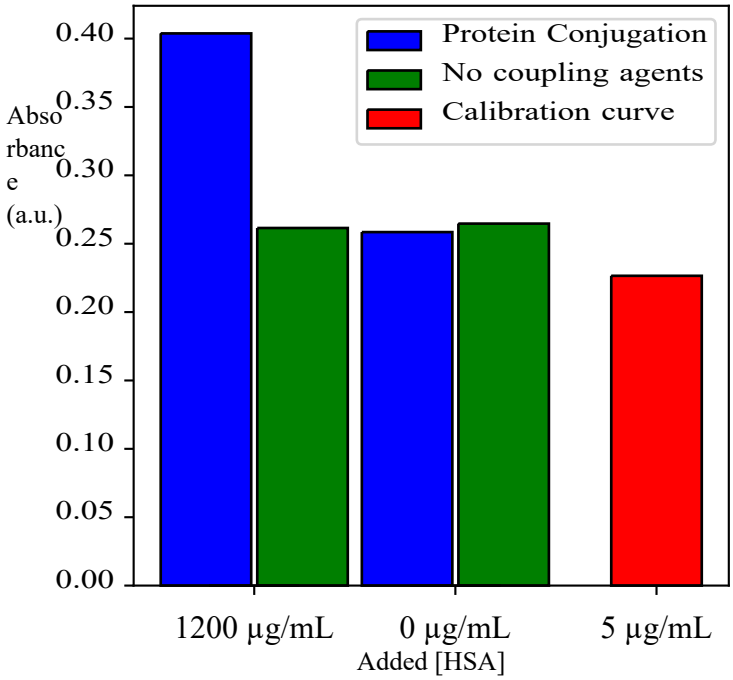

Figure S16: The bar plot indicates the absorbance values obtained with Micro BCA Assay. In blue, the absorbance data of COOH-NPs activated with EDC/NHS then reacted with 1200 or 0 µg/mL of HSA and lastly purified three times with a 0.1 wt% solution of Lutensol AT50 and one time with 2 wt% SDS. In green, the absorbance control data where the COOHNPs were not activated but otherwise treated identically to the blue samples. In red, the absorbance of 5 µg/mL of HSA obtained from the calibration curve data.

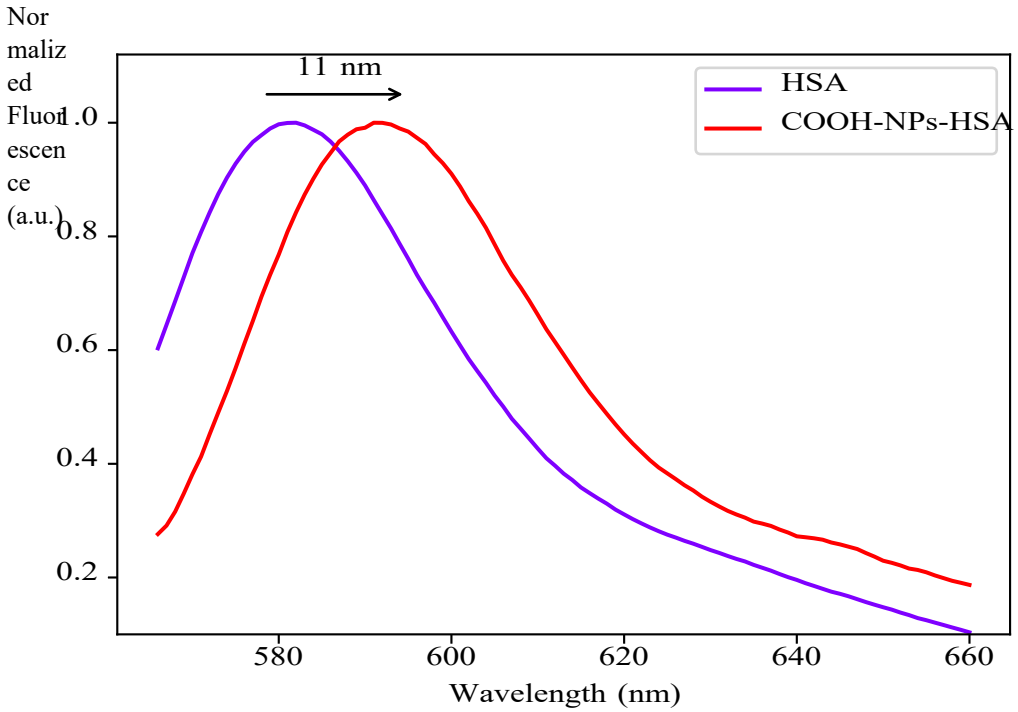

Figure S17: Overlay of HSA-Rhodamine B in DMSO and polymer-HSA-Rhodamine B spectra. The 11 nm red-shift hampers the quantification protocol.

Maximum NPs coverage with HSA

Based on the work of Yu *et al.*,[14] we have assumed that albumin has an equilateral triangular prism volume with the following dimensions: 8 × 8 × 3.5 nm. Overall we will have two faces with a triangle area ($\frac{8\ nm * 6.7\ nm}{2} = 27\ nm$) and three rectangular areas (8 nm ∗ 3.5 nm = 28 nm^2). Assuming a random orientation of the protein on the NPs surface we can average the protein surface area and assume that the protein interacts with a 27.6 nm^2 surface area. Given that our NPs have a diameter of 200 nm, their surface area is 130'000 nm^2. Thus we can calculate how many proteins would fit on the surface area with Equation S7:

$$N\ protein = \frac{Area_{NPs}}{Area_{Protein}} = \frac{130'000}{27.6} = 4'800 \quad \text{(S6)}$$

obtaining approximately 4'800 proteins on each NPs.

From μM concentration to groups per particle

The FGs concentration obtained from the different experiments can be converted to the average number of groups per particle as follows (Equation 11):

$$FGs_{particle} = C * \frac{1}{SC} * \frac{g_{polymer}}{particle} * N_A \tag{11}$$

where *C* is the molar concentration, *SC* is the solid content which in this work was 1*g/L*. The grams of polymer per NPs ($\frac{g_{polymer}}{particle}$) were be calculated with Equation 12:

$$\frac{g_{polymer}}{particle} == V * \rho \tag{12}$$

where *V* is the volume of the NPs treated as a sphere and ρ is the polymer density (1.17 g/L).

References

(1) Chen, Y.; Zhang, Y. Fluorescent quantification of amino groups on silica nanoparticle surfaces. *Analytical and bioanalytical chemistry* 2011, *399*, 2503–2509.

(2) Hsiao, I.-L.; Fritsch-Decker, S.; Leidner, A.; Al-Rawi, M.; Hug, V.; Diabaté, S.; Grage, S. L.; Meffert, M.; Stoeger, T.; Gerthsen, D., et al. Biocompatibility of aminefunctionalized silica nanoparticles: the role of surface coverage. *Small* 2019, *15*, 1805400.

(3) Wang, S. X.; Michiels, J.; Ariën, K. K.; New, R.; Vanham, G.; Roitt, I. Inhibition of HIV virus by neutralizing Vhh attached to dual functional liposomes encapsulating dapivirine. *Nanoscale Research Letters* 2016, *11*, 1–10.

(4) Moser, M.; Nirmalananthan, N.; Behnke, T.; Geißler, D.; Resch-Genger, U. Multimodal cleavable reporters versus conventional labels for optical quantification of accessible amino and carboxy groups on nano-and microparticles. *Analytical chemistry* 2018, *90*, 5887–5895.

(5) Ganachaud, F.; Mouterde, G.; Delair, T.; Elaissari, A.; Pichot, C. Preparation and characterization of cationic polystyrene latex particles of different aminated surface charges. *Polymers for Advanced Technologies* 1995, *6*, 480–488.

(6) Musyanovych, A.; Adler, H.-J. P. Grafting of amino functional monomer onto initiatormodified polystyrene particles. *Langmuir* 2005, *21*, 2209–2217.

(7) Udenfriend, S.; Stein, S.; Boehlen, P.; Dairman, W.; Leimgruber, W.; Weigele, M. Fluorescamine: a reagent for assay of amino acids, peptides, proteins, and primary amines in the picomole range. *Science* 1972, *178*, 871–872.

(8) Wang, C.; Yan, Q.; Liu, H.-B.; Zhou, X.-H.; Xiao, S.-J. Different EDC/NHS activation mechanisms between PAA and PMAA brushes and the following amidation reactions. *Langmuir* 2011, *27*, 12058–12068.

(9) Bharti, S. K., & Roy, R. (2012). Quantitative ^{1}H NMR spectroscopy. *TrAC Trends in Analytical Chemistry*, *35*, 5-26.

(10) Böckenhoff, K., & Fischer, W. (2001). Determination of electrokinetic charge with a particle-charge detector, and its relationship to the total charge. *Fresenius' journal of analytical chemistry*, *371*, 670-674.

(11) Bartczak, D., & Kanaras, A. G. (2011). Preparation of peptide-functionalized gold nanoparticles using one pot EDC/sulfo-NHS coupling. *Langmuir*, *27*(16), 10119-10123.

(12) Zhang, Q., Rui-Xue, L. I., Xin, C. H. E. N., Xing-Xing, H. E., Ai-Ling, H. A. N., Guo-Zhen, F. A. N. G., Ji-Feng L., Shuo, W. A. N. G. (2017). Study of efficiency of coupling peptides with gold nanoparticles. *Chinese Journal of Analytical Chemistry*, *45*(5), 662-667

(13) Monopoli, M. P.; Pitek, A. S.; Lynch, I.; Dawson, K. A. Formation and characterization of the nanoparticle–protein corona. *Nanomaterial Interfaces in Biology: Methods and Protocols* 2013, 137–155.

(14) Yu, S.; Perálvarez-Marín, A.; Minelli, C.; Faraudo, J.; Roig, A.; Laromaine, A. Albumincoated SPIONs: An experimental and theoretical evaluation of protein conformation, binding affinity and competition with serum proteins. *Nanoscale* 2016, *8*, 14393–14405.